

Response to reviewers for the paper “A Systematic Re-evaluation of Methods for Quantification of Bulk Particle-phase Organic Nitrates Using Real-time Aerosol Mass Spectrometry” D.A. Day, P. Campuzano-Jost, B.A. Nault, B.B. Palm, W.W. Hu, H. Guo, P.J. Wooldridge R.C. Cohen, K.S. Docherty, J.A. Huffman, S.S. de Sá, S.T. Martin, J.L. Jimenez

We thank the reviewers for their positive and constructive comments on our paper. To guide the review process we have copied the reviewer comments in black text. Our responses are in regular blue font. We have responded to all the reviewer comments and made alterations to our paper (in bold text).

Reviewer #1

General Comments:

The manuscript by Day et al. compiled an extensive survey of NO_x+ ratios measured for various pRONO₂ compounds and mixtures from multiple AMS instruments, groups, and laboratory and field measurements. They find that the pRONO₂ NO_x+ ratio can be estimated using a ratio referenced to the calibrated NH₄NO₃ ratio (“RoR method”), and explore the basis for quantifying pRONO₂ (and NH₄NO₃) with the RoR method using ground and aircraft field measurements conducted over a large range of conditions. This work will help provide a more consistent and accurate approach to quantification and exploration of bulk particle-phase nitrates in the atmosphere with AMS.

This manuscript is generally well written. Before its publication, the following comments need to be addressed.

Specific Comments:

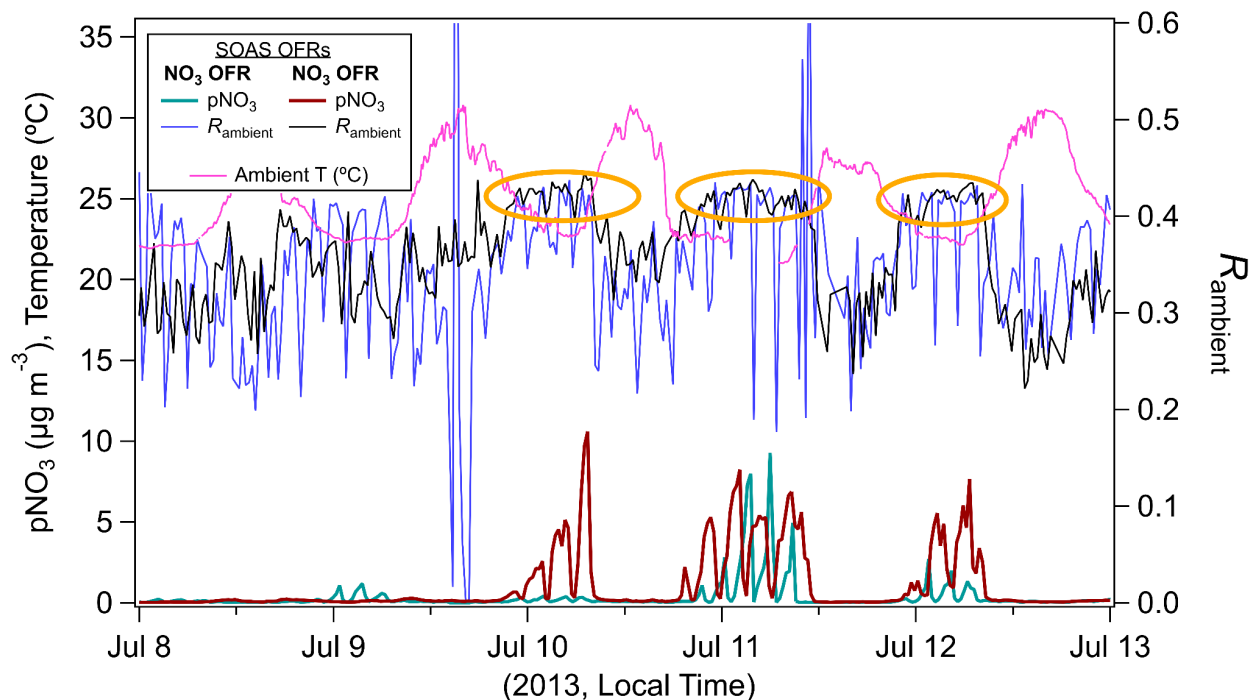
R1.1. The oxidation flow reactor (OFR) measurements are shown in Fig. S9c. What are the oxidants concentrations? It seems that compared with R_{ambient} under the conditions of OH radicals as the oxidant, R_{ambient} is less converged at the calibration RNH₄NO₃ under the conditions of NO₃ radicals. Please elaborate. In addition, Line 340 “Fig. S8c” should be “Fig. S9c”

A1.1 The figure numbering has been corrected. We thank the reviewer for catching that detail.

We can see how Fig. S9c can give the impression that the R_{ambient} for the NO₃-OFR does not converge at $R_{\text{NH}_4\text{NO}_3}$ as closely as data for the OH-OFR does, with increasing pNO₃. In part, that is due to the different scaling of the y-axes. Therefore we have re-scaled all plots in Fig. S9c to the same y-axis values (R_{ambient} : 0-0.6) in the updated manuscript. See new versions copied below. Both OFR types show near perfect convergence, for average quantiles at the higher pNO₃ concentrations where the majority of the higher pNO₃ concentrations were measured

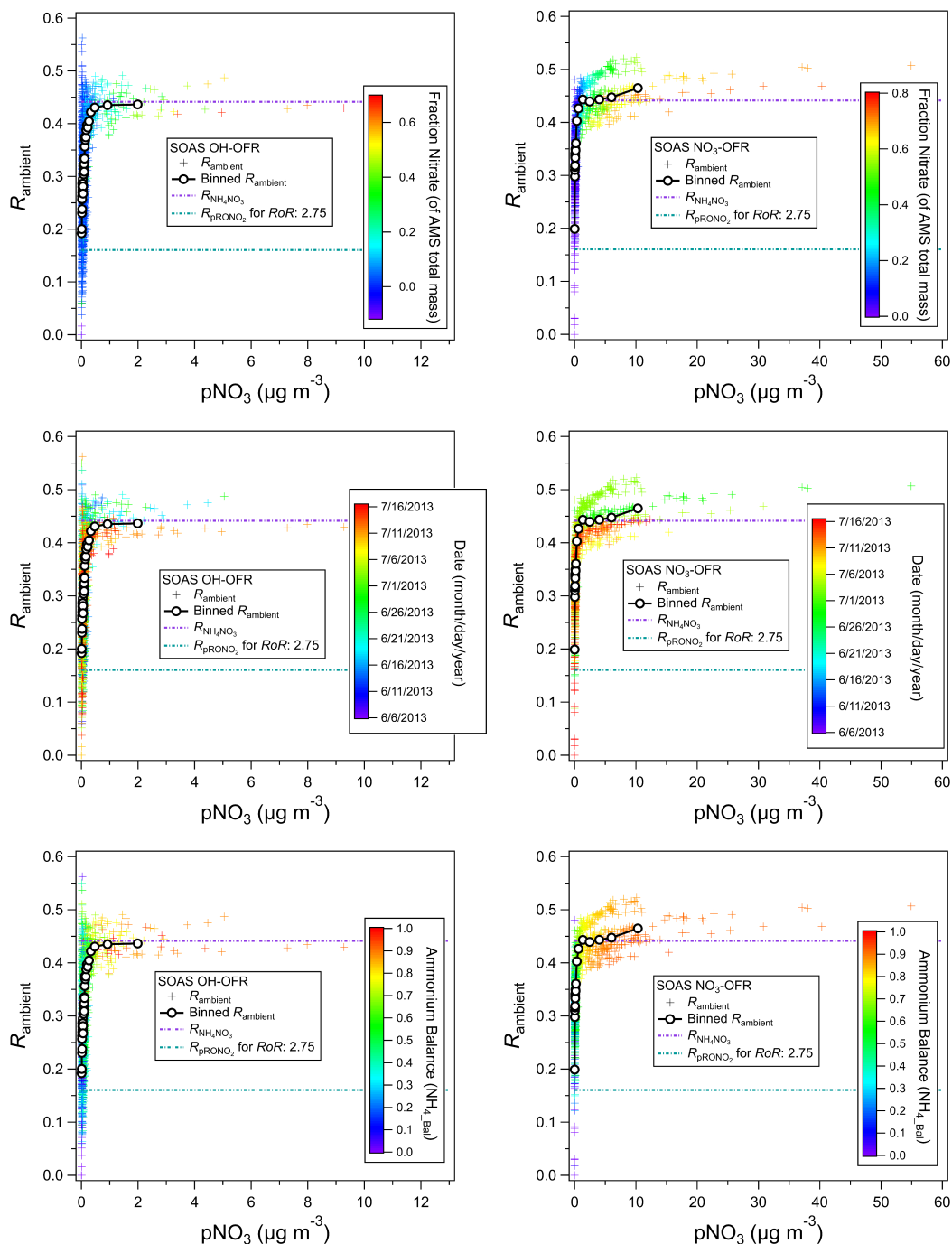
(0.5-2 $\mu\text{g}/\text{m}^3$ for the OH-OFR and 1-6 $\mu\text{g}/\text{m}^3$ for the NO_3 -OFR). Beyond considering the quantile averages, there is a distinct period for the NO_3 -OFR where pNO_3 concentrations increased up to $\sim 10 \mu\text{g}/\text{m}^3$ and reached R_{ambient} of ~ 0.51 , however the OH-OFR was offline during that period, therefore a direct comparison of instrument response with the other OFR cannot be made. For the highest pNO_3 concentrations measured for either OFR mode ($>2 \mu\text{g}/\text{m}^3$ for the OH-OFR and $>10 \mu\text{g}/\text{m}^3$ for the NO_3 -OFR), those consist of three periods for each OFR which do not overlap with each other (in the sense of both falling in those ranges during the same sampling period) and with two sets above and one set below the average $R_{\text{NH}_4\text{NO}_3}$ line (for each OFR mode) — as seen in the middle row of Fig. S9c, colored by time. Overall, these differences are on order of the $\pm 5\%$ variability of the 9 calibration $R_{\text{NH}_4\text{NO}_3}$ measured throughout the campaign.

To more directly assess any systematic differences of R_{ambient} at elevated pNO_3 for the two OFR modes, we inspected the time series to compare NO_x^+ ratios during periods when both OFRs showed substantially elevated pNO_3 . During those periods, the R_{ambient} for both OFRs peaked at values with indistinguishable differences. See the time series below highlighting three nights where both OFRs showed substantial pNO_3 production (with comparison periods marked by orange ovals). Note that periodic decreases in the R_{ambient} (more strongly seen for the OH-OFR) are due to the intentional oxidant exposure cycling. Also a couple noisy periods for the OH-OFR R_{ambient} (mid-day on July 9 and 11) are simply due to very low pNO_3 values, since the R_{ambient} values are not screened for detection limits here.



The oxidant exposures for the OH-OFR were cycled through multiple levels every few hours ranging from $\sim 10^{10}$ to $\sim 10^{13}$ molecules $\text{OH cm}^{-3} \text{s}$ (~ 0.1 –40 equivalent days of ambient OH aging), as shown for this same dataset in Hu et al. (2016) (Fig. 6 in that manuscript). The

NO₃-OFR was run similarly to the data analyzed in Palm et al. (2017) where NO₃ radical exposures range from $\sim 2 \times 10^{11}$ to 8×10^{12} molecules NO₃ cm⁻³ s (~ 0.1 -4 equivalent days of ambient NO₃ aging, see Figs. 5,6 in Palm et al. (2017)). However, the large NH₄NO₃ in both OFR modes occurred nearly exclusively during nighttime when temperature decreased to ~ 20 -23 °C and relative humidity (RH) climbed to >90-95% and generally required just moderate amounts of OH or NO₃ exposure. In both cases, the aerosol formation may have been driven by some commonalities including lower T, high RH, and desorption of ammonia from the OFR surfaces, while the presumed HNO₃ formation required may have been formed from different mechanisms (NO₂ oxidation for the OH-OFR and N₂O₅ hydrolysis for the NO₃-OFR). Regardless, given that large amounts of NH₄NO₃ were formed in both OFR modes, it is not surprising that they show similar NO_x⁺ ion ratio responses. That said, it supports that any differences in oxidation of other components (e.g., the OA and SOA components) do not appear to affect the response of mixed NH₄NO₃, which is the main purpose of including this dataset in the manuscript.



“Figure S9c. R_{ambient} vs $p\text{NO}_3$ for SOAS campaign for oxidation flow reactor (OFR) measurements using OH (left column) and NO_3 (right column) radicals as oxidants. Each of the three rows contains the same data, but colored by different measures: mass fraction of AMS mass that is aerosol nitrate (top row), time (middle row), and NH_4_{Bal} (bottom row) as indicated in colorbar legends. Data is overlaid with quantile averages (medians). NH_4_{Bal} is calculated as the molar ratio of $\text{NH}_4/(\text{NO}_3+2\times\text{SO}_4)$. Values approaching unity suggests full ion balance of sulfate and nitrate by ammonium and little contribution of organic nitrate or organic sulfate. Lower values suggest acidic particles and/or the presence of substantial organic nitrate or organic sulfate. Horizontal lines are shown for calibration $R_{\text{NH}_4\text{NO}_3}$ and corresponding estimated R_{pRONO_2} (from $\text{RoR} = 2.75$).”

R1.2. I appreciate the summary of results for studies using PMF for pRONO₂ separation with AMS in Table S4. I suggest adding the contributions of OA factors to pRONO₂ in another table/figure which is sorted by OA factors, so that readers can see the OA factors' contributions clearly.

A1.2 We are pleased to hear that the referee found the PMF summary table to be valuable. We are hesitant to further generalize the associations and contributions between pRONO₂ and PMF factors, beyond the brief summaries already in column 6, in this manuscript. Column 6 is meant to provide a general idea of the types of PMF factors that pRONO₂ has been associated with and relative amounts as reported specifically by each separate study. Simply compiling them according to factor identities would lack important context considering the variety of approaches, factors resolved, and study conditions (i.e., field/lab, season, sampling location). Thus, while we appreciate the reviewer's suggestion and agree such a synthesis would be valuable, we expect that proper representation could be on the scope of another manuscript and/or large portion therein. We note that our descriptions and synthesis of the many other studies using the NO_x⁺ ratio method here in this manuscript generally does not go beyond brief summaries and discussion of details specifically in the context of evaluating the analytical methods.

R1.3. How is R_{ambient} detection limit calculated? Please elaborate.

A1.3. We assume the reviewer is referring to the detection limit screening mentioned in the caption of Fig. 4 stating "...for all data as well as only when above the R_{ambient} detection limit (DL)." We have added clarification to the caption:

"...for all data as well as only when above the R_{ambient} detection limit (DL; approximated as when both NO_x⁺ ions are above standard AMS detection limits (Drewnick et al., 2009))."

A detailed analysis of uncertainties using the NO_x⁺ ratio method, including approaches to applying detection limits, are the subject of a forthcoming manuscript.

R1.4. More cites need to be listed to support the conclusions in line 535-545.

A1.4 We have added several references supporting the statements in this passage and have made a few edits to provide additional clarification. It now reads:

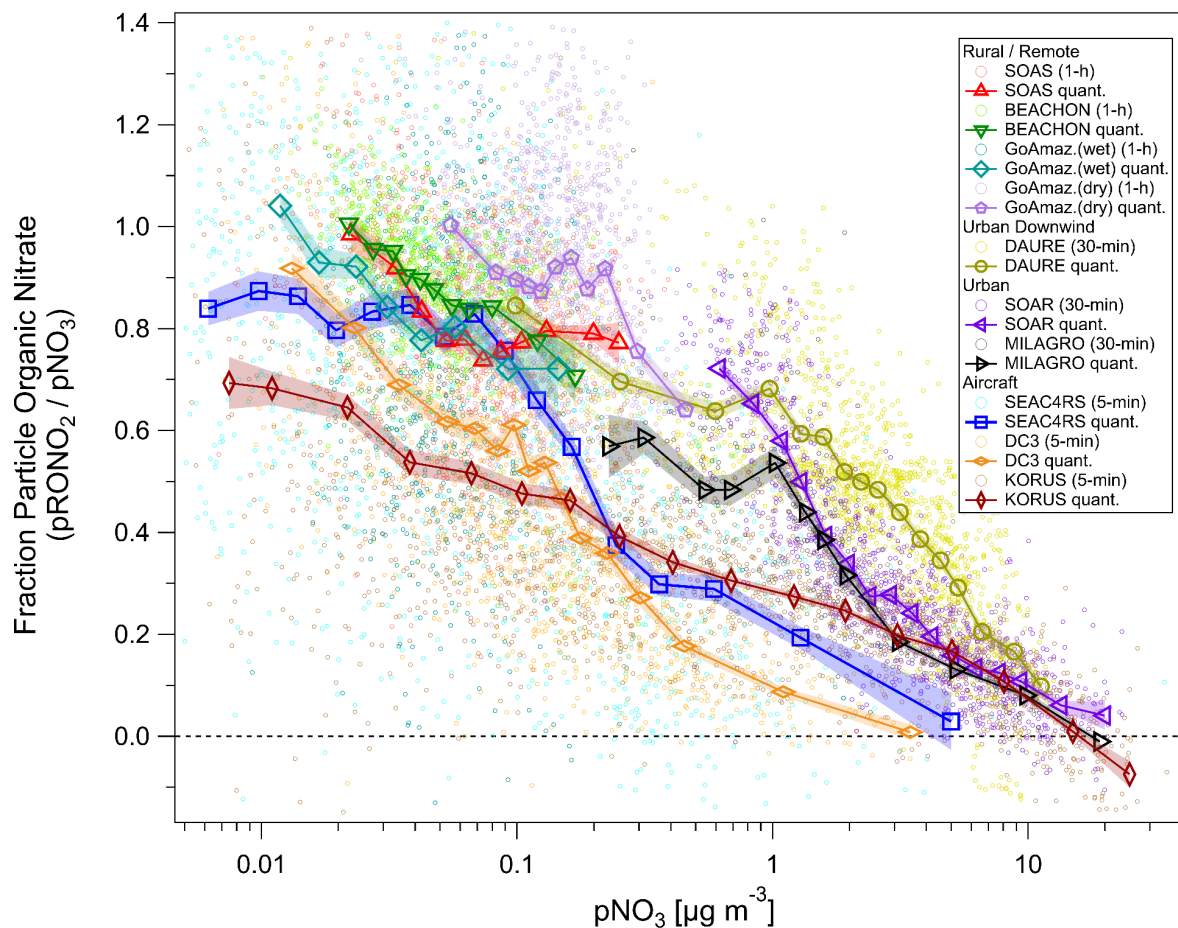
"A few other notable trends and observations are as follows (with details provided in Sects. S3, S4). PMF-resolved pRONO₂ often tends to have the largest contribution from (and association with) LO-OOA/SV-OOA, followed by MO-OOA/LV-OOA, especially for biogenically-influenced locations (Sun et al., 2012; Hao et al., 2014; Xu et al., 2015; Zhang et al., 2016; Kortelainen et al., 2017; Yu et al., 2019; Sect. S3, Table S4). That is consistent with pRONO₂ forming in fresh SOA (i.e. LO-OOA/SV-OOA) and being partly lost as the OA ages and/or MO-OOA/LV-OOA consisting of a mix of aged OA, some of which was not associated with pRONO₂. Nitrate associated with aged ambient BBOA can be dominated

by NH_4NO_3 (shown with aircraft data using PMF in this study, and discussed more broadly in Nault et al. (2021)); however, primary and secondary pRONO₂ (or other oxidized organic nitrogen) associated with BBOA emission has been reported in the laboratory and field, sometimes as large contributions (Tiitta et al., 2016; Reyes-Villegas et al., 2018; McClure et al., 2020; Lin et al., 2021). When NH_4NO_3 factors are resolved, they tend to contain substantial contributions (~15–80%) of OA (non-NO_x⁺) ions (Sun et al., 2012; Hao et al., 2014; Xu et al., 2015; Zhang et al., 2016; Kortelainen et al., 2017). Generally, those non-NO_x⁺ contributions seem to be higher for strongly biogenically-influenced measurements and less so during cooler wintertime periods when NH_4NO_3 comprises a larger fraction of nitrates (Xu et al., 2015; this study).”

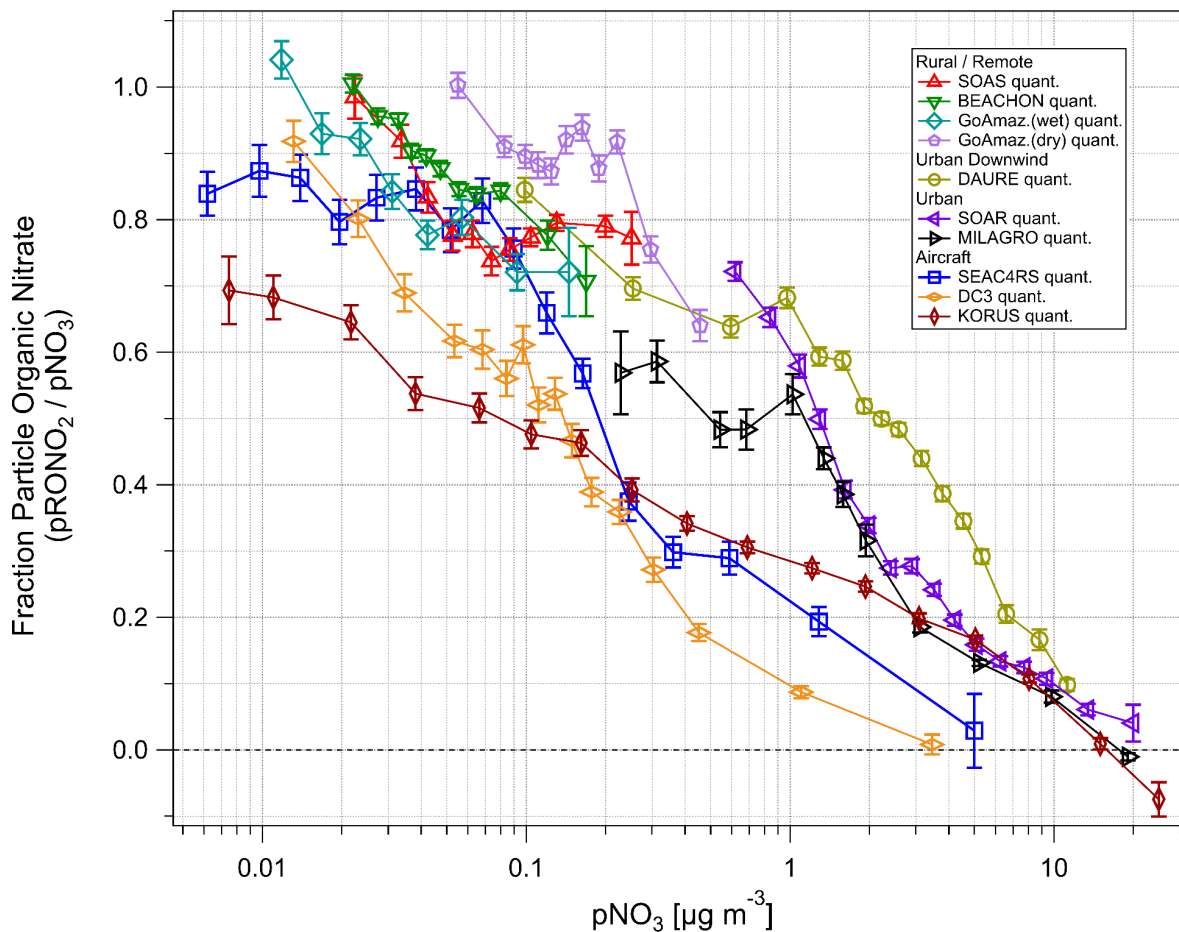
We have also added text on pertinent methods and results from the recently published Lin et al., (2021) paper (see C.2 below).

R1.5. Fig. 5: It would be better to add error bars to show the uncertainty or scatter of the data. Otherwise, we don't know how significant the fraction variations are.

A1.5 This is a good point. We have added the standard errors for the quantile averages (as shaded swaths), which shows that the trends are highly significant. Nearly all error bars are not much larger than the markers. We also have included a version in the SI that excludes the non-binned average datapoints and shows the standard errors with more traditional error bar format for an alternate simplified rendering of the quantile standard errors (and also slightly zoomed). Both versions are copied below.

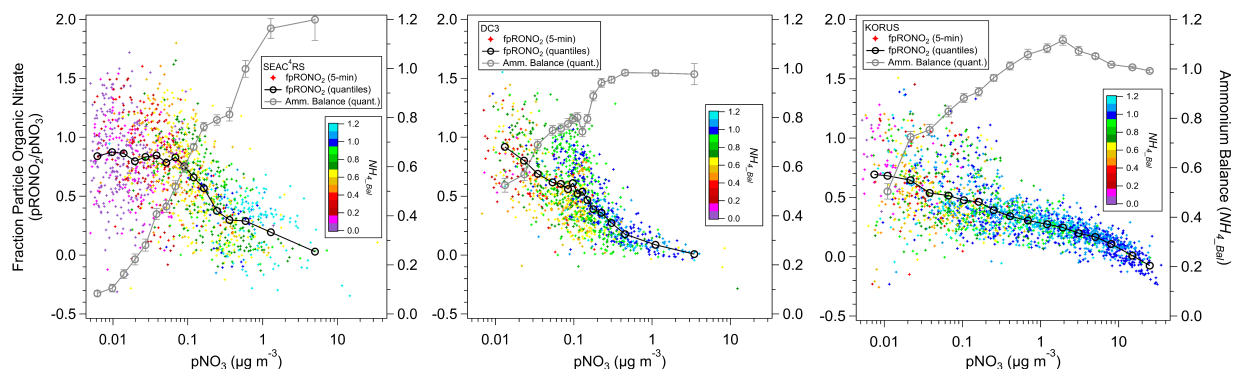


“Figure 5. Fraction of total non-refractory submicron nitrate that is organic ($f_{p\text{PRONO}_2}$) vs. total nitrate concentration ($p\text{NO}_3$) for several ground and aircraft campaigns. Campaigns span: late-winter to summer across the northern hemisphere and wet/dry seasons near the equator; from ground level to the upper troposphere; and urban to remote locations. NO_x^+ ion signals were first averaged and then data was conservatively screened for detection limits ($S/N > 1-3$) using both NO_x^+ ions (small circles). Quantile averages (means, 7–15 bins) are also shown for each campaign. Additionally, for all campaigns, one additional average was calculated and included with the quantile averages for the highest 1% (3%) of $p\text{NO}_3$ for urban/aircraft (rural/remote) campaigns in order to extend the $p\text{NO}_3$ by a factor of $\sim 1.3-3$ (undersampled chemical regime, but with sufficiently high S/N). The average of the lowest 3% of $p\text{NO}_3$ for the MILAGRO campaign is also included. Shaded swaths indicate the standard error for the quantile averages. Many are no larger than the markers and thus may not be very apparent. See Fig. S31 for a version showing a simplified version with only binned averages and standard error bars.”



“Figure S31. Same as Fig. 5 except that non-binned data are not shown, standard errors are shown as traditional error bars, gridlines are added, and it is slightly zoomed.”

We also updated Fig. S30 to now similarly include standard error bars of quantile averages for the ammonium balance:



“Figure S30. f_{pRONO2} vs. pNO_3 for aircraft campaigns (5-min, quantile averages). 5-min f_{pRONO2} is colored by ammonium balance (NH_4_{Bal} , molar ion charge ratio of NH_4^+ to $NO_3^- + SO_4^{2-}$) and quantile averages and standard errors of NH_4_{Bal} are also shown. At lower pNO_3 , NH_4_{Bal} was much lower for SEAC⁴RS compared to the other campaigns, while DC3 was slightly lower than for KORUS.”

R1.6. Fig. S17 and S25: Consider using logarithmic coordinates.

A1.6 Immediately below are versions of the two panels in Fig. S17 with the y-axis shown as log scale. Also below them are the linear versions from the submitted preprint for comparison. Upon inspection, we feel that when shown as log scale, the key features are de-emphasized with no additional useful information conveyed. I.e. the comparison of the relative tightness/diffuseness of the distributions and values for each factor are obscured (main point). The only new information that is brought forward are the comparisons of 1's and 0's occurrences for the IEPOX-SOA in the left (bootstrapping) panel, which is not an important detail (and can technically be seen in the linear scale). Thus, we prefer to keep them as linear scale in the manuscript. We do note that we post all of our figures and data for our published manuscripts for public access, should such finer details be of interest to future researchers.

Fig. S17 with log y-axis
(note that all zeros are converted to 0.5 in order to display on log scale)

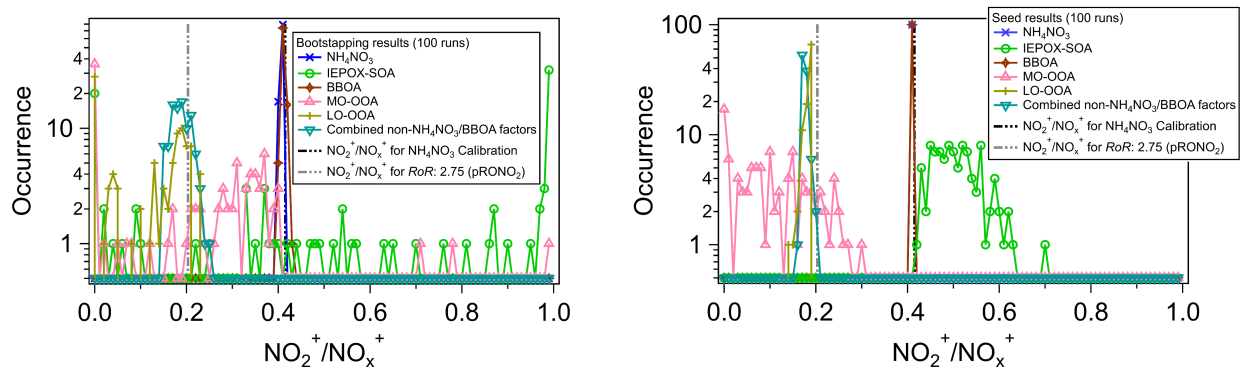
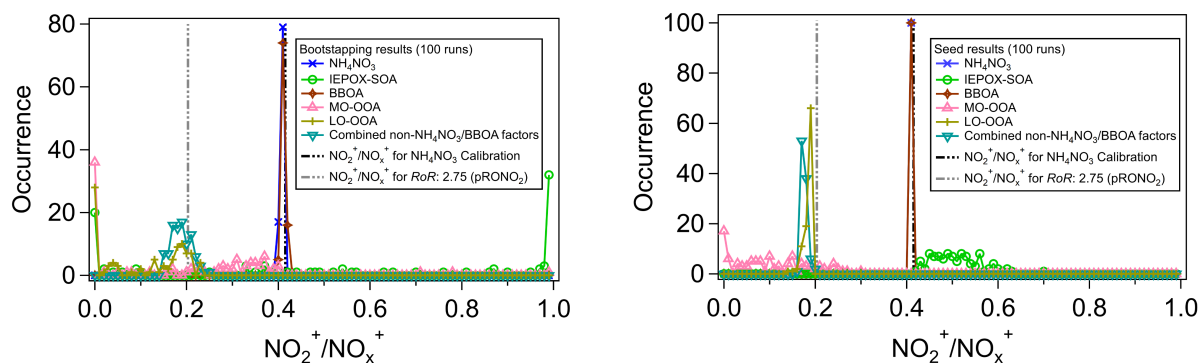


Fig. S17 with linear y-axis (currently in manuscript)



Reviewer #2

General Comments:

Day et al. provide a comprehensive, and likely exhaustive, review of studies which have used AMS measurements to derive the relative concentrations of organic and inorganic nitrate aerosols from a suite of laboratory-based, ground-based, and aircraft-based research campaigns. This paper appears to be very carefully researched and written and will become an important resource for future investigators wishing to use AMS data to quantify organic nitrates.

Day et al. first review and evaluate the existing datasets that can offer insight into the capabilities of AMS data for distinguishing organic and inorganic nitrates. This leads to the primary conclusion that a reasonably simple analysis using the AMS data (so-called “RoR” analysis) can usefully differentiate these chemically distinct classes of nitrate aerosols. Further, the RoR analysis is applied to data from a suite of previous campaigns and then used to argue that organic nitrates are an increasingly important fraction of aerosol nitrate in cleaner environments, almost everywhere where AMS measurements have occurred. This is a significant conclusion that may direct future research.

There is no question to me that this paper deserves publication in AMT and I recommend publication following very minor revisions and consideration for a few points.

R2.1 The primary question that I have for the authors to consider is whether they have sufficiently demonstrated that variations in the NO_x^+ ratios are overwhelmingly due to the relative importance of inorganic and organic nitrates. For example, the result in Figure 5 could in principle be explained by a simple variation in the NO_x^+ ratio from pure NH_4NO_3 as a function of the NH_4NO_3 concentration. Or perhaps a matrix effect could play a role where the relative ion signals changes depending on the fraction of total aerosol mass that is NH_4NO_3 relative to e.g. organics. I did not see it sufficiently argued here that one of these could not be the explanation. It would be nice for example to see a laboratory measurement of the NO_x^+ ratio as a function of NH_4NO_3 , both from pure or internally mixed aerosols. I expect that in one of the cited papers this has already been shown, and I would suggest drawing some attention to that and clearly stating it in this work.

A2.1. The reviewer brings up a good point. As stated in Sect. 3, Line 270, we are preparing a separate manuscript detailing the uncertainties in application of the NO_x^+ ratios and *RoR* methods for apportionment and quantification of nitrate with AMS. That topic includes too much new analysis and discussions to include in this manuscript, which is already quite extensive. In that manuscript, we systematically explore effects on NO_x^+ ratios for NH_4NO_3 and pRONO_2 from varying concentration and matrices (mixed with OA, inorganics), in the laboratory and field, and show that under typical ambient sampling conditions, effects, if present, are small. We expect that paper to be submitted soon.

Nonetheless, we believe there is sufficient evidence presented in this manuscript that the trends in NO_x^+ ratios are indeed consistent with a continuum of inorganic/organic nitrate contributions and not consistent with matrix or concentration effects. We address this point directly with the following new text (added as a new section prior to the conclusion):

“Section 8: Further discussion of the efficacy and support for NO_x^+ ratio apportionment

From simply inspecting the relationships of f_{pRONO_2} and NO_x^+ ratios vs pNO_3 in Figs. 5 and S9, or the variability of ratios shown in Fig. 2, it could be postulated that such trends could simply be driven by changing pNO_3 concentrations or some other confounding factor such as matrix effects. Thus, here we review several pieces of evidence presented in this manuscript and prior literature that, taken together, provide overwhelming support that the variability of measured R_{ambient} between the calibrated $R_{\text{NH}_4\text{NO}_3}$ and the R_{OR} -derived R_{pRONO_2} values is dominantly controlled by the continuum of $\text{NH}_4\text{NO}_3/\text{pRONO}_2$ contributions. We emphasize that this discussion is relevant only to conditions where refractory nitrates (NaNO_3 , $\text{Ca}(\text{NO}_3)_2$, e.g., from dust or seasalt) or nitrites are not substantial components of the aerosol, since they produce different NO_x^+ ratios and the apportionment equation becomes underconstrained.

Kiendler-Scharr et al., (2016) present laboratory data of NO_x^+ ratios for over a range of NH_4NO_3 concentrations and mixtures (Sect. S1, Fig. S1 in that paper). They conclude that “fragmentation behaviour as a function of mass concentration, composition of the particles and particle size of NH_4NO_3 and mixtures of NH_4NO_3 with $(\text{NH}_4)_2\text{SO}_4$ and glutaric acid, were observed to be constant, independent of mass concentration down to $0.1 \mu\text{g}/\text{m}^3$ in the laboratory aerosol”. We regularly generate scatterplots of the two NO_x^+ ions over a range of NH_4NO_3 concentrations recorded during calibrations. This is the typical method we use and recommend for quantifying the $R_{\text{NH}_4\text{NO}_3}$ and inspecting for any irregularity in the relationships (such as non-linearity). The insensitivity of $R_{\text{NH}_4\text{NO}_3}$ with concentration is a consistent feature. We have systematically explored concentration and matrix effects of NH_4NO_3 and pRONO_2 in the laboratory and with field data and show that under typical ambient conditions, matrix effects, if present, are small. This will be discussed in a future manuscript exploring the uncertainties of these apportionment and quantifications methods. We note that this result contrasts with a similar study that assessed the viability of apportioning inorganic and organic sulfate using H_ySO_x^+ and SO_x^+ ion ratios (Schueneman et al., 2021). Strong dependencies on aerosol composition (i.e. acidity and nitrate mass fraction, but generally not OA concentration) were found for those ions, making sulfate apportionment not possible under a substantial fraction of conditions found in the atmosphere. We speculate that the much lower volatility of inorganic sulfate compared to nitrate may play a role in this difference.

Inspection of the NO_x^+ ratios vs pNO_3 shown in Fig. S9a for the three urban field studies shows that ratios generally plateau at $R_{\text{NH}_4\text{NO}_3}$ when the nitrate is only ~30% of the bulk aerosol — and thus still dominated by other compounds — supporting that mixing with other complex ambient components does not alter the NO_x^+ ratio produced from NH_4NO_3 . Furthermore, at lower pNO_3 , NO_x^+ ratios for all campaigns generally approach expected pRONO_2 ratios. While this certainly does not prove that at the lower pNO_3

range, the nitrates are primarily organic, and primarily NH_4NO_3 at the higher pNO_3 range, such consistent behavior would be highly coincidental. We also point to the comparisons of AMS-apportioned pRONO_2 with independent measurements of total RONO_2 , shown in Figs. 3, S12a. There is a high level of tracking between the two independent organic nitrate components, while flying through intermittent elevated nitrate plumes, which were sometimes correlated with elevated OA while in other cases not (Figs. S11, S12b). This provides strong evidence that the use of NO_x^+ ratios are indeed effectively apportioning nitrate, and changing non-nitrate fractions are not hindering the method. Similarly, the apportioned NH_4NO_3 tracks well with estimates of NH_4 not associated with sulfate for those same aircraft flights (Figs. S11, S12b).

Finally, the exploration of NO_x^+ ratio apportionment with PMF, shows the distinct signature of pRONO_2 NO_x^+ ratios for secondary OA factors and that of NH_4NO_3 for the other components (Figs. S17, S25). That result would be highly unlikely if the continuum of NO_x^+ ratios in the total aerosol were dominantly controlled by concentration or matrix artifacts. While this preponderance of evidence strongly supports the effectiveness of this method, further laboratory and field data studies and analyses, including instrument comparisons, should be conducted to better constrain uncertainties and improve the method.”

Specific points:

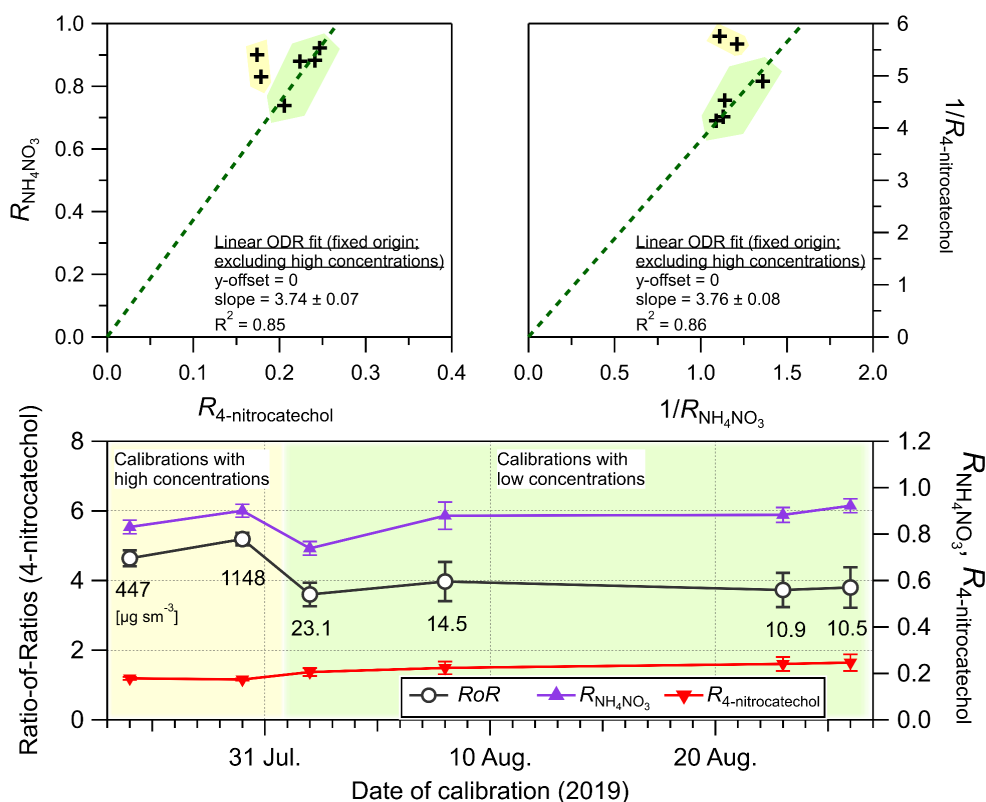
R2.2. Line 252: The idea that a mechanism for variability in the NO_x^+ ratio might be understood by studying it systematically with the same instrument is somewhat refuted by the FIREX observations (Fig S5) where a wide range was observed for both NO_x^+ ratios with no known variability in instrument operation.

Fig S5 actually shows a lot of instability in the RoR, and that the NO_x^+ ratios from 4-nitrocatechol and NH_4NO_3 are poorly correlated from day-to-day, or that there may be some anti-correlation. One thing I find problematic here is that the uncertainties indicated for each measurement do not represent the range of all the values measured. That is, the precision of the RoR measurement from any short period of time seems a lot better than the day-to-day variability in the measurement of this parameter, meaning that significant variability in ambient NO_x^+ ratio might be observed without a change in the real ratio of $\text{RONO}_2 / \text{NO}_3^-$. I realize that these measurements were performed on a nitro compound rather than an organic nitrate, but it's not made clear that this would matter. My expectation also is that since this experimental group is probably the most experienced and meticulous of those who use AMS, this represents the best-case scenario for AMS NO_x^+ ratio stability. Overall, it would be nice to have some comment here or elsewhere on what this tells us about the uncertainty in the derived RONO_2 and NO_3^- concentrations.

A2.2. We thank the reviewer for bringing this to our attention. That figure was added toward the end of drafting this manuscript and did not receive the level of scrutiny it should have. It included several calibrations where there were not back-to-back 4-nitrocatechol (4-NC) and NH_4NO_3 calibrations. This can be very problematic when the AMS instrument has been recently turned

on since NO_x^+ ratios can be a very sensitive parameter in the AMS and can take several hours to stabilize. Given that this was an aircraft campaign, the instrument was turned on/off every day, including the pumping on the mass spectrometer (for flights and ground-service days). Therefore, we have now limited the data shown to only calibrations where the instrument was on for several hours and there were back-to-back 4-NC and NH_4NO_3 calibrations (which is limited to post-flight calibrations). We also draw attention to the effect where very high 4-NC calibration concentrations were sampled. The properly screened data show more typical stability in $R_{\text{NH}_4\text{NO}_3}$ (relative standard deviation: $\pm 11\%$) and correlation with the $R_{4\text{-nitrocatechol}}$.

The revised figure and updated caption, including discussion of some of these points, are copied below:



“Figure S5. NO_x^+ ratios for 4-nitrocatechol (4-NC) and NH_4NO_3 and the corresponding R_{oR} for 4-NC measured on board the NASA DC-8 during the FIREX-AQ biomass burning study (Pagonis et al., 2021). Values listed below the R_{oR} data points are the concentrations of 4-NC used to calibrate. While some calibrations were performed during pre-flight (4-NC only), post-flight (4-NC and NH_4NO_3), and ground-service days (4-NC and NH_4NO_3), only data for post-flight are shown. The reason for including only post-flight calibrations is: 1) due to the fact that typically the instrument had not been operating long enough (only a couple hours) to produce stable NO_x^+ ratios, which can be a sensitive parameter and require substantial time to stabilize shortly after starting up the AMS; 2) NH_4NO_3 calibrations were never conducted pre-flight (only 4-NC for cross calibration of sensitivity between the AMS and another chemical instrument, EESI — see Pagonis et al. (2021)); and 3) often the 4-NC and NH_4NO_3 calibrations were not conducted in close temporal proximity on ground-service days and/or too soon after startup for ratios to stabilize. Scatter plots

are shown for both the standard $R_{\text{NH}_4\text{NO}_3}$ vs $R_{4\text{-nitrocatechol}}$ format (as $\text{NO}_2^+/\text{NO}^+$, top left) and as inverse ratios (top right), showing good correlation, over the limited range. Note that the calibrations conducted early in the campaign at very high 4-NC concentrations (indicated in yellow) are not included in the statistics here, nor for those in Fig. S4 and Table S2. This is because we have observed that when sampling very high OA concentrations ($>50\text{-}200 \mu\text{g m}^{-3}$), NO_x^+ ratios can be substantially skewed. This will be discussed in detail in a forthcoming manuscript exploring uncertainties of the nitrate apportionment methods. Similar behavior was also observed for H_ySO_x^+ and SO_x^+ ion ratios when sampling inorganic sulfate (Schueneman et al., 2021). While this dataset suggests that a similar *RoR* relationship may be applicable to 4-NC and possibly other nitro organics or nitroaromatics, the number of datapoints (4), compounds (1), and instruments (1), as well as the range in $R_{\text{NH}_4\text{NO}_3}$, are very limited. Therefore it is not clear if NO_x^+ ratios for nitro compounds generally have a well-defined *RoR* and track NH_4NO_3 ratios. Further work would be required to draw any general conclusions, ideally including more compounds and mixtures, under different conditions, and with different instruments. To our knowledge, this provides the first example of repeated calibrations of a compound that produces NO_x^+ ions throughout a campaign, directly showing tracking of the NO_x^+ ratios with those of NH_4NO_3 . Thus, it represents some indirect support for application of the *RoR* method to a single instrument throughout a campaign to apportion pRONO_2 and NH_4NO_3 .”

The values for 4-NC were also updated in Table S2 and Fig. S4.

R2.3. Line 293: “was” -> “were”

A2.3 Corrected

R2.4. Line 458: FPEAK appears here for the first time and is not well explained. Please define this.

A2.4. Added definition as rotation parameter.

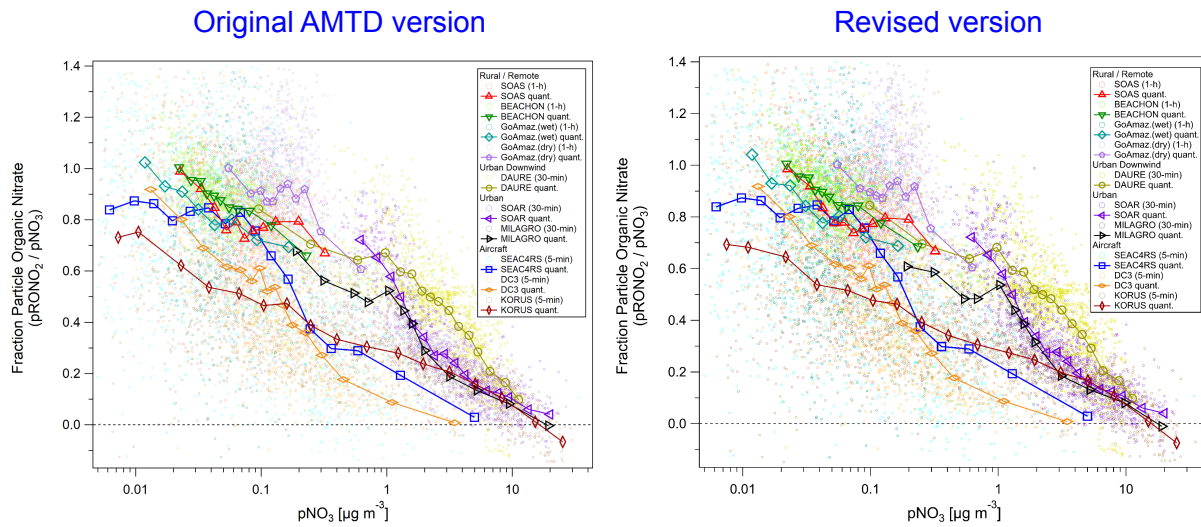
R2.5. Section 7 / figure 5: It may make sense to remind the reader of the method used here to quantify pRONO_2 and the $\text{pRONO}_2 / \text{pNO}_3$ ratio, after all the discussion of *RoR* vs. PMF methods.

A2.5. Good suggestion. Added prominently as second sentence in that section:
“**The apportionment was conducted using the *RoR* method.**”

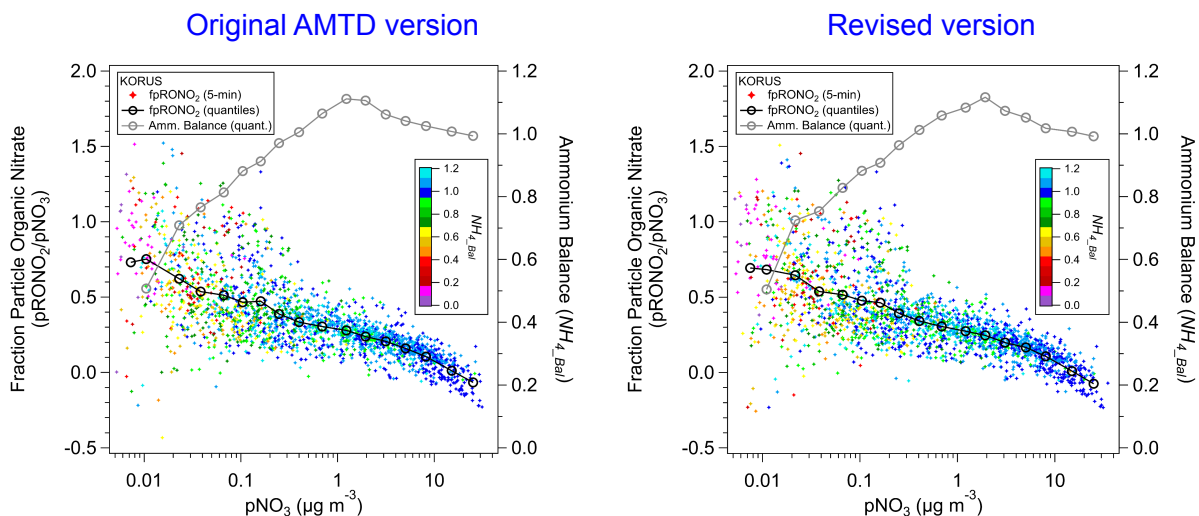
Additional Changes

A few additional changes were made to the manuscript (small corrections, added clarity, new references, figure formatting tweaks), which were all minor, and do not significantly alter any discussions or conclusions. They are as follows:

C.1 A small improvement was made to the quantile binning code used to generate Fig. 5 which was applied only to the DC3 and SEAC⁴RS data for the submitted AMTD version. In the updated manuscript, the improved quantile binning was applied to the other campaigns, resulting in subtle, small shifts in the pNO_3 -binning centerpoint datapoints and generally less than a few percent in f_{pRONO_2} , with no alteration to overall trends. The coding improvement involved excluding pNO_3 points where f_{pRONO_2} data was not present in order to ensure that quantile bins have the same number of valid datapoints, as intended. Original AMTD and revised version are copied below (both in original AMTD format without error bars for direct comparison).



Since the revised f_{pRONO_2} is also included in the Fig. S30 plot panel showing KORUS data, that plot was also revised. Similarly the ammonium balance quantiles were re-averaged with the updated function with very minor changes. Original AMTD and revised version are copied below.



C.2 Since the submission of this preprint, a study by Lin et al. (2021) was published that uses the NO_x^+ ratio and PMF methods to apportion AMS nitrate, thus we have included reference to the study in a few places in the revised manuscript and text describing the methods and results relevant to this manuscript in sections describing PMF applications (Sects. 5.2.1, S3; Table S4). The updated text and table are as follows:

Introduction: two Lin et al. (2021) references added.

Sect. 5.2.1:

“Lin et al. (2021) conducted PMF using only the NO_x^+ ions and nitro-polycyclic aromatic hydrocarbon (NPAH) ions.”

Sect. S3

“Lin et al. (2021) conducted PMF using only the NO_x^+ ions and 16 nitro-polycyclic aromatic hydrocarbon (NPAH, markers of combustion) ions fitted in the soot particle aerosol mass spectrometer (SP-AMS) spectrum for field measurements conducted in NW China during November. Three factors were resolved and assigned as inorganic nitrate, secondary organic nitrate, and primary organic nitrate. During a haze period the inorganic nitrate factor comprised 80% of the pNO_3 , with 17% and 3% attributed to the secondary and primary organic nitrate factors, respectively. During the “reference period” (outside of haze events), those fractions were 47%, 36%, and 17%, respectively. The NO_x^+ ratios for the factor profiles resolved were 0.77 (0.72), 0.34 (0.28), and 0.15 (0.09) for two different approaches used (unconstrained and constrained PMF), respectively. Thus, taking the inorganic nitrate factor NO_x^+ ratio as equivalent to the $R_{\text{NH}_4\text{NO}_3}$ (which was stated to be similar), the secondary organic nitrate factor ratio has a *RoR* of 2.3 (2.6), while the primary organic nitrate would be much higher (5.1, 8.0). It is not clear if the AMS nitrate signal from the factor assigned as primary organic nitrate is comprised of organic nitrates, nitroaromatics and/or other NO_x^+ ion-producing compounds. Combustion source studies conducted in the laboratory showed that NO_x^+ ratios for lubricant oil and coal were similar to the inorganic nitrate ratios, while biomass burning produced NO_x^+ ratios were similar to the secondary organic nitrate factor ratios. The constrained PMF approach involved constraining all the NPAH ion signals to the primary organic nitrate factor, and was used for the main scientific analyses. The NO_x^+ ratio method was also conducted to separate inorganic and organic nitrate using a range of R_{pRONO_2} , 0.1-0.34 (0.1 per Kiendler-Scharr et al. (2016) and 0.34 representing the constrained PMF-resolved secondary organic nitrate factor), representing *RoR* of 7.7-2.3. Organic nitrate concentrations calculated using $R_{\text{pRONO}_2} = 0.34$ agreed well with the PMF apportionment (PMF vs NO_x^+ ratio method regression slope: 0.88), while using $R_{\text{pRONO}_2} = 0.1$ did not (PMF vs NO_x^+ ratio method regression slope: 0.46), consistent with using a *RoR* values recommended in this manuscript.”

Table S4:

Reference	Sample description	No. fact. ^a	$R_{\text{NH}_4\text{NO}_3}$ comp ^b	f_{pRONO_2} ^c	pRONO ₂ factors ^d	RoR ^e	NO _x ⁺ ratio meth. ^f
Lin et al. (2021)	NW China, November	3	“within range”	20%, 53% (haze, non-haze)	Secondary pRONO ₂ (17, 36%) Primary pRONO ₂ + NPAH (3,17%) (haze, non-haze)	Secondary pRONO ₂ (2.3-2.6) Primary pRONO ₂ + NPAH (5.1-8.0)	Yes

(only column labels and new row added to revised manuscript shown here)

C.3 The average value and standard deviation of $R_{\text{NH}_4\text{NO}_3}$ for KORUS-AQ was added to the Fig. S9a caption with the additional text now reading:

“Where only one $R_{\text{NH}_4\text{NO}_3}$ is shown, only one value was available for the data period shown (MILAGRO) or they are averages of several stable values (see Fig. 2 for averages and standard deviations for SOAS and BEACHON, and KORUS-AQ was 0.97 ± 0.04).”

C.4 We added statements to the abstract and introduction clarifying that all analysis presented here is for the “standard vaporizer”, not the “capture vaporizer” in order to avoid any confusion, since our group has published several papers on characterizing and using the capture vaporizer.

Added to Abstract:

“All data and analysis presented here is for using the standard AMS vaporizer.”

Added to Introduction:

“All data, analysis, and recommendations presented here is for use with the *standard* AMS vaporizer; while in practice, similar methods could be applied to explore the possibility of using data from an AMS equipped with the *capture* vaporizer to apportion nitrate, although it would likely have higher detection limits (Hu et al., 2017).”

C.5 Figures in the main manuscript were slightly revised including: increasing and standardizing some font sizes for readability, adding panel letters, and removing unneeded duplicate axes. Revised versions are included in the revised manuscript.

References Cited:

Drewnick, F., Hings, S. S., Alfarra, M. R., Prevot, a. S. H. and Borrmann, S.: Aerosol quantification with the Aerodyne Aerosol Mass Spectrometer: detection limits and ionizer background effects, *Atmospheric Measurement Techniques*, 2(1), 33–46, 2009.

Hao, L. Q., Kortelainen, A., Romakkaniemi, S., Portin, H., Jaatinen, A., Leskinen, A., Komppula,

- M., Miettinen, P., Sueper, D., Pajunoja, A., Smith, J. N., Lehtinen, K. E. J., Worsnop, D. R., Laaksonen, A. and Virtanen, A.: Atmospheric submicron aerosol composition and particulate organic nitrate formation in a boreal forestland–urban mixed region, *Atmos. Chem. Phys.*, 14(24), 13483–13495, 2014.
- Hu, W., Palm, B. B., Day, D. A., Campuzano-Jost, P., Krechmer, J. E., Peng, Z., de Sá, S. S., Martin, S. T., Alexander, M. L. L., Baumann, K., Hacker, L., Kiendler-Scharr, A., Koss, A. R., de Gouw, J. A., Goldstein, A. H., Seco, R., Sjostedt, S. J., Park, J.-H., Guenther, A. B., Kim, S., Canonaco, F., Prévôt, A. S. H., Brune, W. H. and Jimenez, J. L.: Volatility and lifetime against OH heterogeneous reaction of ambient isoprene-epoxydiols-derived secondary organic aerosol (IEPOX-SOA), *Atmos. Chem. Phys.*, 16(18), 11563–11580, 2016.
- Hu, W., Campuzano-jost, P., Day, D. A., Croteau, P., Canagaratna, R., Jayne, J. T., Worsnop, D. R., Jimenez, J. L., Hu, W., Campuzano-jost, P., Day, D. A., Croteau, P., Canagaratna, R., Jayne, J. T., Worsnop, D. R. and Jimenez, J. L.: Evaluation of the new capture vaporizer for aerosol mass spectrometers (AMS) through field studies of inorganic species, *Aerosol Sci. Technol.*, 51(6), 735–754, 2017.
- Kiendler-Scharr, A., Mensah, A. A., Friese, E., Topping, D., Nemitz, E., Prevot, A. S. H., Äijälä, M., Allan, J., Canonaco, F., Canagaratna, M., Carbone, S., Crippa, M., Dall'Osto, M., Day, D. A., DeCarlo, P., Di Marco, C. F., Elbern, H., Eriksson, A., Freney, E., Hao, L., Herrmann, H., Hildebrandt, L., Hillamo, R., Jimenez, J. L., Laaksonen, A., McFiggans, G., Mohr, C., O'Dowd, C., Otjes, R., Ovadnevaite, J., Pandis, S. N., Poulain, L., Schlag, P., Sellegri, K., Swietlicki, E., Tiitta, P., Vermeulen, A., Wahner, A., Worsnop, D. and Wu, H.-C.: Organic nitrates from night-time chemistry are ubiquitous in the European submicron aerosol, *Geophys. Res. Lett.*, 43(14), 7735–7744, 2016.
- Kortelainen, A., Hao, L., Tiitta, P., Jaatinen, A., Miettinen, P., Kulmala, M., Smith, J. N., Laaksonen, A., Worsnop, D. R. and Virtanen, A.: Sources of particulate organic nitrates in the boreal forest in Finland, *Boreal Environ. Res.*, 22, 13–26, 2017.
- Lin, C., Huang, R.-J., Duan, J., Zhong, H. and Xu, W.: Primary and Secondary Organic Nitrate in Northwest China: A Case Study, *Environmental Science & Technology Letters*, doi:10.1021/acs.estlett.1c00692, 2021.
- McClure, C. D., Lim, C. Y., Hagan, D. H., Kroll, J. H. and Cappa, C. D.: Biomass-burning-derived particles from a wide variety of fuels – Part 1: Properties of primary particles, *Atmos. Chem. Phys.*, 20(3), 1531–1547, 2020.
- Nault, B. A., Campuzano-Jost, P., Day, D. A., Jo, D. S., Schroder, J. C., Allen, H. M., Bahreini, R., Bian, H., Blake, D. R., Chin, M., Clegg, S. L., Colarco, P., Crouse, J., Cubison, M. J., DeCarlo, P. F., Dibb, J., Diskin, G. S., Hodzic, A., Hu, W., Katich, J. M., Kim, M. J., Kodros, J., Kupc, A., Lopez-Hilfiker, F. D., Marais, E. A., Middlebrook, A., Neuman, J. A., Nowak, J. B., Palm, B. B., Paulot, F., Pierce, J., Schill, G. P., Scheuer, E., Thornton, J. A., Tsigaridis, P. R., Wennberg, P. O., Williamson, C. J. and Jimenez, J. L.: Models underestimate the increase of acidity with remoteness biasing radiative impact calculations, *Communications Earth & Environment*, 2(93), doi:10.1038/s43247-021-00164-0, 2021.
- Pagonis, D., Campuzano-Jost, P., Guo, H., Day, D. A., Schueneman, M. K., Brown, W. L., Nault, B. A., Stark, H., Siemens, K., Laskin, A., Piel, F., Tomsche, L., Wisthaler, A., Coggon, M. M., Gkatzelis, G. I., Halliday, H. S., Krechmer, J. E., Moore, R. H., Thomson, D. S., Warneke, C., Wiggins, E. B. and Jimenez, J. L.: Airborne extractive electrospray mass spectrometry

measurements of the chemical composition of organic aerosol, *Atmos. Chem. Phys.*, 14(2), 1545–1559, 2021.

Palm, B. B., Campuzano-Jost, P., Day, D. A., Ortega, A. M., Fry, J. L., Brown, S. S., Zarzana, K. J., Dube, W., Wagner, N. L., Draper, D. C., Kaser, L., Jud, W., Karl, T., Hansel, A., Gutiérrez-Montes, C. and Jimenez, J. L.: Secondary organic aerosol formation from in situ OH, O₃, and NO₃ oxidation of ambient forest air in an oxidation flow reactor, *Atmos. Chem. Phys.*, 17(8), 5331–5354, 2017.

Reyes-Villegas, E., Priestley, M., Ting, Y.-C., Haslett, S., Bannan, T., Le Breton, M., Williams, P. I., Bacak, A., Flynn, M. J., Coe, H., Percival, C., Allan, J. D., Breton, M. L., Attribution, Creative Commons, Reyes-Villegas, E., Reyes-Villegas, E. and By, C. C.: Simultaneous aerosol mass spectrometry and chemical ionisation mass spectrometry measurements during a biomass burning event in the UK : insights into nitrate chemistry, *Atmos. Chem. Phys.*, 18(6), 4093–4111, 2018.

Schueneman, M. K., Nault, B. A., Campuzano-Jost, P., Jo, D. S., Day, D. A., Schroder, J. C., Palm, B. B., Hodzic, A., Dibb, J. E. and Jimenez, J. L.: Aerosol pH indicator and organosulfate detectability from aerosol mass spectrometry measurements, *Atmos. Meas. Tech.*, 14(3), 2237–2260, 2021.

Sun, Y. L., Zhang, Q., Schwab, J. J., Yang, T., Ng, N. L. and Demerjian, K. L.: Factor analysis of combined organic and inorganic aerosol mass spectra from high resolution aerosol mass spectrometer measurements, *Atmos. Chem. Phys.*, 12(18), 8537–8551, 2012.

Tiitta, P., Leskinen, A., Hao, L., Yli-Pirilä, P., Kortelainen, M., Grigonyte, J., Tissari, J., Lamberg, H., Hartikainen, A., Kuusalo, K., Kortelainen, A.-M. M., Virtanen, A., Lehtinen, K. E. J., Komppula, M., Pieber, S., Prévôt, A. S. H., Onasch, T. B., Worsnop, D. R., Czech, H., Zimmermann, R., Jokiniemi, J. and Sippula, O.: Transformation of logwood combustion emissions in a smog chamber: formation of secondary organic aerosol and changes in the primary organic aerosol upon daytime and nighttime aging, *Atmos. Chem. Phys.*, 16(20), 13251–13269, 2016.

Xu, L., Suresh, S., Guo, H., Weber, R. J. and Ng, N. L.: Aerosol characterization over the southeastern United States using high-resolution aerosol mass spectrometry: spatial and seasonal variation of aerosol composition and sources with a focus on organic nitrates, *Atmos. Chem. Phys.*, 15(13), 7307–7336, 2015.

Yu, K., Zhu, Q., Du, K. and Huang, X.-F.: Characterization of nighttime formation of particulate organic nitrates based on high-resolution aerosol mass spectrometry in an urban atmosphere in China, *Atmos. Chem. Phys.*, 19(7), 5235–5249, 2019.

Zhang, J. K., Cheng, M. T., Ji, D. S., Liu, Z. R., Hu, B., Sun, Y. and Wang, Y. S.: Characterization of submicron particles during biomass burning and coal combustion periods in Beijing, China, *Sci. Total Environ.*, 562, 812–821, 2016.